NUMERICAL STUDY OF A WIND TURBINE WITH CROSS-FLOW RUNNER

Andrei DRAGOMIRESCU[1]

Majoritatea turbinelor eoliene clasice nu pot demara la viteze ale vântului scăzute, de 2-3 m/s. Altele, aşa cum este Savonius, au un randament maxim redus, care le face inutile în condiţii de vânt slab. Prin urmare, noi tipuri de turbine sunt necesare pentru a utiliza energia vântului chiar şi atunci când viteza lui este scăzută. În această lucrare, o turbină eoliană cu rotor transversal este studiată cu metode numerice pentru a-i estima performanţele. Rezultatele obţinute sugerează că această turbină are un moment de demaraj ridicat iar coeficientul de putere maxim este comparabil cu cele ale turbinelor eoliene cu ax orizontal. Pe baza rezultatelor obţinute concepţia turbinei poate fi îmbunătăţită pentru creşterea în continuare a performanţelor.

Most of the classical wind turbines are not able to start at wind speeds as low as 2-3 m/s. Other turbines, like Savonius, have a low maximum efficiency, rendering them useless in poor wind conditions. Therefore, new turbine designs are required to harvest wind power even when the wind speed is low. A wind turbine having a crossflow runner is studied numerically in this work in order to estimate its performance. The results obtained suggest that this turbine has a considerable high starting torque and its maximum power coefficient is comparable to those of horizontal axis wind turbines. Based on the results obtained, the design can be improved to further increase turbine performance.

Keywords: crossflow runner, power coefficient, starting torque, torque coefficient, wind turbine

1. Introduction

Small wind turbines are usually located where the generated power is required, and not necessarily where the wind resource is best. For such turbines, the minimum wind speed, at which the turbine runner starts rotating, and the starting torque become essential parameters. These parameters depend on the type of the turbine (with horizontal or vertical axis), number of blades, etc. Thus, according to the experimental data presented by Wright and Wood [1], a small, three-bladed, horizontal axis wind turbine can start at an average wind speed of about 4.6 m/s. Vertical axis wind turbines (VAWT) of Savonius type can start at lower wind speeds, down to about 2 m/s, but they have a poor efficiency, the power coefficient, C_p, being less than 0.25. Other VAWT, namely the Darrieus type, are not self-starting

[1] Lecturer, Faculty of Power Engineering, University Politehnica of Bucharest, e-mail: dragomirescu@hydrop.pub.ro

at all in normal conditions, unless they have variable pitch blades, a solution which, however, makes the turbine impractical for small applications. Nevertheless, the usage of wind turbines in areas with average wind velocities in the range of 2-3 m/s or even lower could be desired or required, usually coupled with other non-conventional energy generators (like solar panels), to supply isolated houses, GSM stations, etc. Considering the limitations of classical wind turbine types, new turbine designs should be sought in order to meet the demands in poor wind conditions.

As a solution for low wind speeds, Mandiş et al. [2] propose a wind turbine derived from a Banki water turbine, i.e. a turbine with a crossflow runner. The usage of a nozzle is also suggested. However, no considerations regarding the performance of such a turbine are made. Furthermore, although the nozzle will clearly improve the turbine performance, it will increase the size of the turbine and it will require an additional device for pointing the turbine into the wind.

In this article, we examine the extent to which a wind turbine with crossflow runner can be used for extracting wind energy in poor wind conditions. Before starting the study, some considerations were taken into account. To make the operation independent of wind direction, the axis should be vertical and the runner should not be covered by any nozzle or casing. However, the axis can be also horizontal when the turbine is placed on a rooftop in order to take advantage of the fact that the roof acts as a wind concentrator. In this second situation the usage of a casing could come into discussion. As a first case study, a free crossflow runner placed in a low speed air flow was investigated by numerical simulations. The study aimed at assessing the starting torque, the variations of the torque and power coefficients and the range of tip speed ratios, in which the operation is possible. The computations were performed with the finite volumes method implemented in the commercial code Fluent.

2. Problem description

The geometry of the crossflow runner, presented in Fig. 1, is the one typical for a Banki runner. The design of the runner is thoroughly described in literature [2, 3]. As outer diameter we chose $D_1 = 1\,000$ mm. With this, the radial rim width $a = 170$ mm and the inner diameter $D_2 = 660$ mm resulted. The blades are circular arcs with the radius $R_b = 146.8$ mm. Their centers lie on a circle of radius $R_c = 361.2$ mm. The aperture of a blade is $\theta_b = 17.55°$. The number of blades, z, was chosen so that the angle between two adjacent blades, γ, equals roughly the aperture. It resulted $z = 20$ blades and $\gamma = 18°$.

It was considered that the runner is placed in a free air flow and there are no obstacles or wind concentrators in its vicinity. Due to the fact that the runner has the same geometry in any cross-section, only 2D simulations were performed.

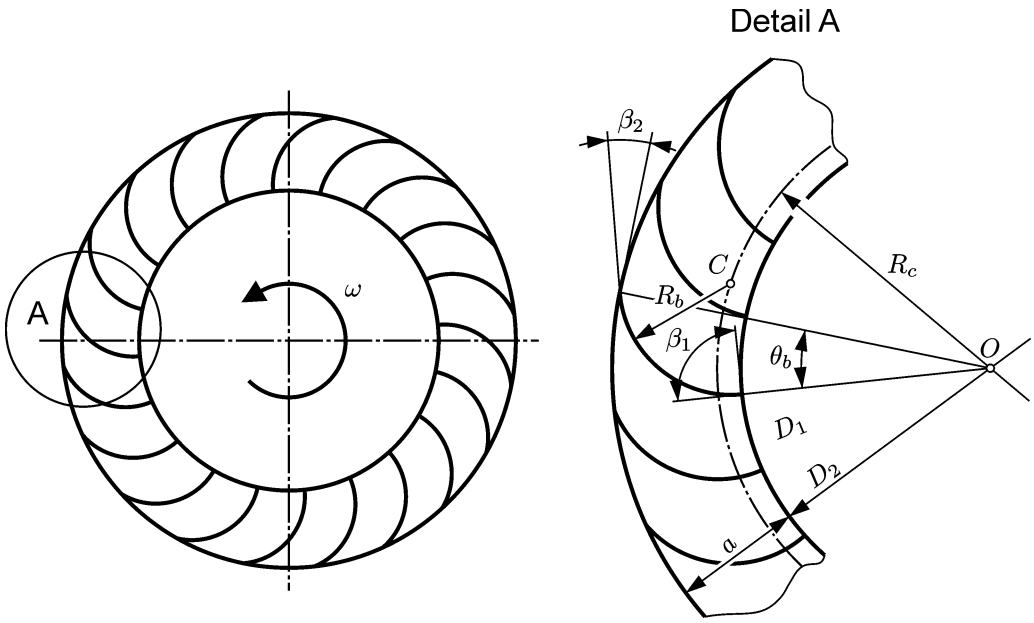

Fig. 1. Geometry of the crossflow runner.

The computational domain was chosen as a rectangle having a width of 5 m and a length of 10 m. The runner was placed along the symmetry axis of this domain at a distance of 2.5 m from the upstream boundary.

There are several methods for simulating the flow outside and inside the moving runner. Among them, the sliding mesh technique was chosen, because it is the most realistic, allowing to investigate the complex effects of the unsteady flow on the blades and in the wake of the runner. The computational domain was split into two subdomains: a rotating one, containing the runner, and a fixed one, containing the exterior. Both subdomains were meshed with unstructured meshes consisting in triangular control volumes, except for the vicinity of the blades, where rectangular boundary elements were used. The meshes were created so that the control volumes are finer near the blades and coarser towards the boundaries. The two meshes are separated by interfaces, which allow the transport of the flow properties as described in literature [4]. A sketch of the computational domain is presented in Fig. 2.

All the simulations were performed for a wind speed $v_\infty = 2$ m/s, considering the reference pressure $p_0 = 10^5$ Pa and the reference temperature $\vartheta_0 = 15^\circ\mathrm{C}$ (absolute reference temperature $T_0 = 288.15$ K). At the reference conditions the density and dynamic viscosity of air are $\varrho = 1.2084$ kg/m^3 and $\eta = 1.7979 \cdot 10^{-5}$ Pa·s, respectively. The air was considered incompressible. Several cases were investigated, for tip speed ratios between 0 (cogged runner)

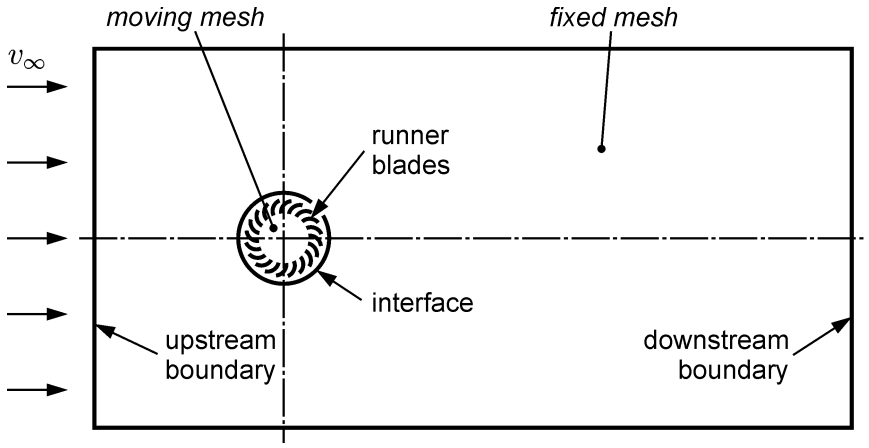

Fig. 2. Computational domain.

Table 1

Parameters of the simulations

λ	ω [rad/s]	n [rot/min]	T [s]	T_b [s]	f_b [Hz]
0	0	0	–	–	–
0.1	0.4	3.82	15.708	0.785	1.27
0.2	0.8	7.64	7.854	0.393	2.55
0.3	1.2	11.46	5.236	0.262	3.82
0.4	1.6	15.28	3.927	0.196	5.09
0.5	2.0	19.10	3.142	0.157	6.37
0.6	2.4	22.92	2.618	0.131	7.64

and 0.6. In our problem the tip speed ratio is defined by the relationship

$$\lambda = \frac{\omega R_1}{v_\infty}, \tag{1}$$

where ω is the angular velocity of the runner. Values of some parameters of the simulations (angular velocity ω, rotational speed n, period T of a full rotation, time T_b in which the angle between two succesive blades is swept, frequency f_b corresponding to T_b) are summarized in Table 1. It should be specified that the runner rotates counterclockwise.

The continuity and momentum equations were solved together with those of the realizable k-ϵ (RKE) turbulence model, a model which was found to assure convergence.

On the upstream boundary a constant velocity of 2 m/s (i.e. v_∞) was imposed, while on the other boundaries a relative static pressure of 0 Pa was set. On the blades (solid walls) the usual no-slip condition was imposed. The time step used remained the same for all simulations: 0.01 s.

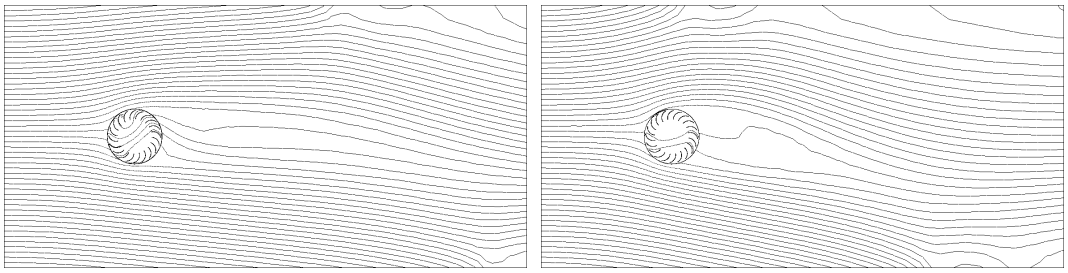

Fig. 3. Streamlines obtained at two tip speed ratios: a) $\lambda = 0.1$, b) $\lambda = 0.5$.

As convergence criterium for each time step, the one recommended for technical applications was employed, namely the drop of all scaled residuals below 10^{-3} [4]. For each tip speed ratio, the simulation advanced in time until a stabilization of the moment coefficient around an average value was observed for more than 30 s of the simulation time (more than 3 000 time steps).

The first simulation was performed for $\lambda = 0$. The solution obtained in the last time step was used as initial guess at the next tip speed ratio, $\lambda = 0.1$. For the other tip speed ratios a similar procedure was applied. Not only this procedure assured a better convergence in the first time steps of each simulation, but it also corresponded to the real turbine operation, in which, under the condition of a constant wind speed, the rotational speed of the runner, cogged initially, raises gradually until it stabilizes itself at a value that assures a balance between the power of the air current and the power transmitted by the turbine shaft.

3. Results

Fig. 3 presents streamlines obtained at two tip speed ratios. It can be seen that, along the wind direction, the air current drifts in a direction opposite to the runner movement. The drift is not significant but it becomes more important as the tip speed ratio increases. The streamlines suggest the appearance of vortices in the wake. However, the vortices do not develop but are rappidly destroyed by the main flow, as it is suggested in Fig. 4 by the velocity vectors plotted in the wake at two different time moments. The time difference between the plots is 2 s, which we consider enough to highlight the behaviour of the vortices. The explanation for the low vorticity downstream of the turbine could reside in the fact that the air that crosses the runner generates at the exit small air jets that hinders the forming of a "dead water" zone, which, in case of bluff bodies, is the source of vortices.

Fig. 5 shows vectors of absolute velocity inside the runner obtained at tip speed ratios ranging from 0.1 to 0.5. These vectors make evident the double interaction between the air current and the runner, this double interaction being

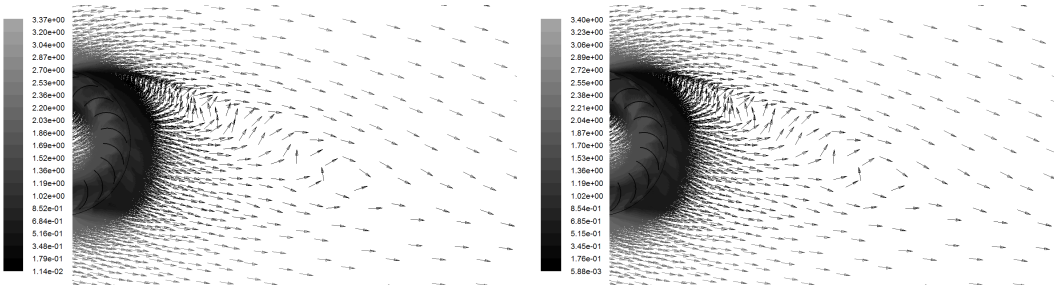

Fig. 4. Velocity vectors in the wake of the runner obtained for $\lambda = 0.5$, plotted at a time interval of 2 s.

actually a characteristic of crossflow runners. A first interaction between air and blades takes place upstream, when the air enters into the runner. Then, the flow crosses the vaneless interior of the runner and a second interaction occurs downstream, when the air exits. A vortex can be observed inside the runner. Its size remains small up to $\lambda = 0.3$. Above this value of the tip speed ratio, the size of the vortex increases rapidly and for $\lambda = 0.5$ it occupies almost half of the inner space. The growth of the vortex diminishes the effective flow section so that the flow rate, which crosses the runner and interacts with the blades, is expected to decrease. The plots also suggest that, up to $\lambda = 0.3$, a positive interaction (an interaction that generates a driving torque) exists between the flow and approximately nine blades placed to the left and down and, respectively, to the right and up in the plots. On another eight blades (to the left and up), the interaction has a braking effect on the runner. The remaining blades, about three (to the right and down), can be considered as idle. As the inner vortex grows, at $\lambda = 0.4$ and $\lambda = 0.5$, it can be observed a decrease of the number of blades, on which the flow has a positive action. Consequently, the performance of the turbine is expected to deteriorate at higher tip speed ratios.

Time variations of torque coefficients obtained at tip speed ratios between 0 and 0.5 in the last 30 s of each simulation time are presented in Fig. 6. Since the simulations were made in a two-dimensional space, the values of the coefficients were calculated considering a unit height of the runner. The following relationship was used [5]:

$$c_m = \frac{M}{0.25\,\varrho\,v_\infty^2\,D_1\,S}\,, \tag{2}$$

where M is the torque acting on the blades extracted from the simulations at each time step, and the area S is given by the relationship $S = D_1\,H$ with $H = 1$ being the unit height of the runner. It can be seen that by cogged runner ($\lambda = 0$) the torque coefficient is practically constant and has a value close to 3.6. This unexpected high value denotes a very good starting torque, which allows an easy

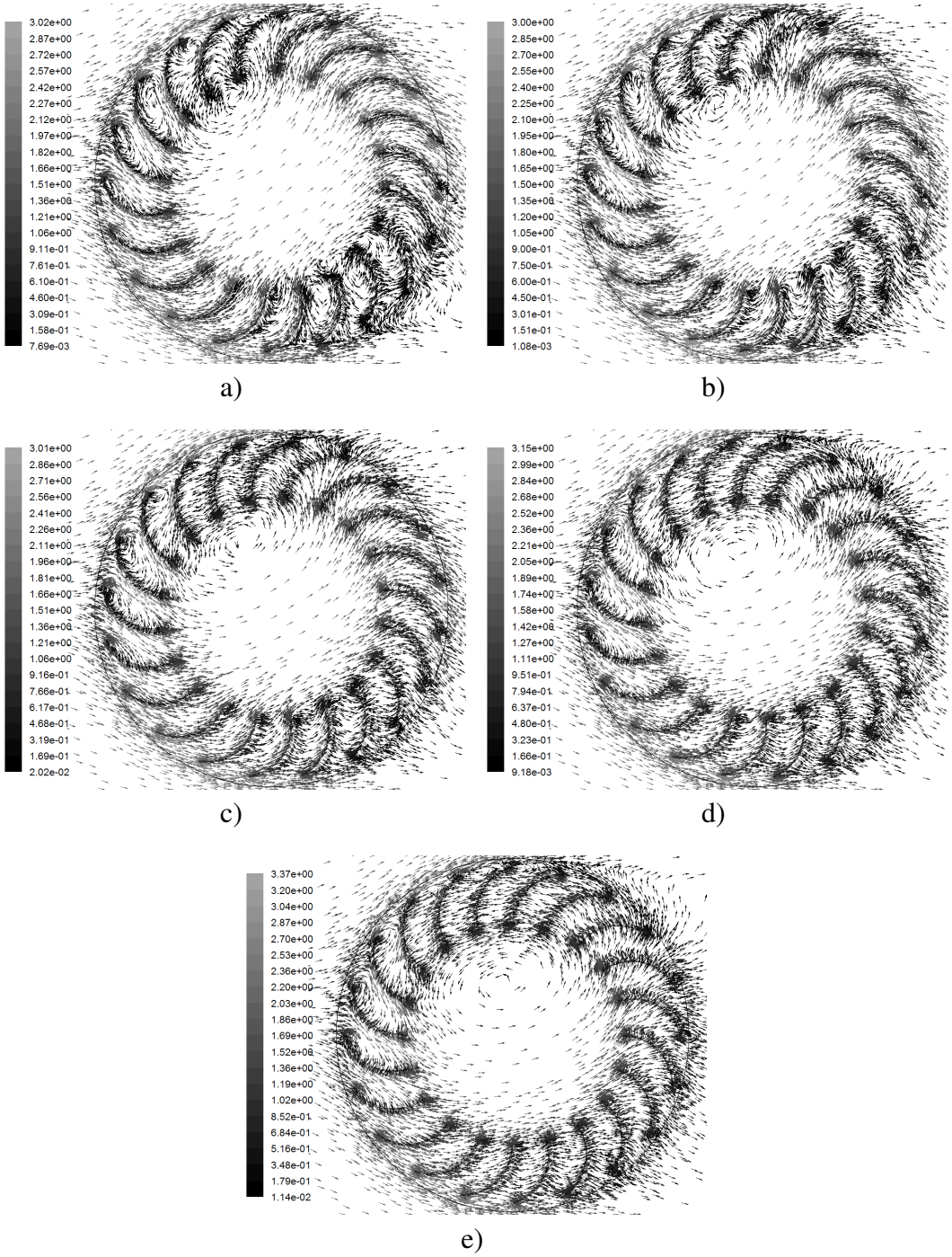

Fig. 5. Vectors of absolute velocity inside the runner for different tip speed ratios: a) $\lambda = 0.1$, b) $\lambda = 0.2$, c) $\lambda = 0.3$, d) $\lambda = 0.4$, and e) $\lambda = 0.5$.

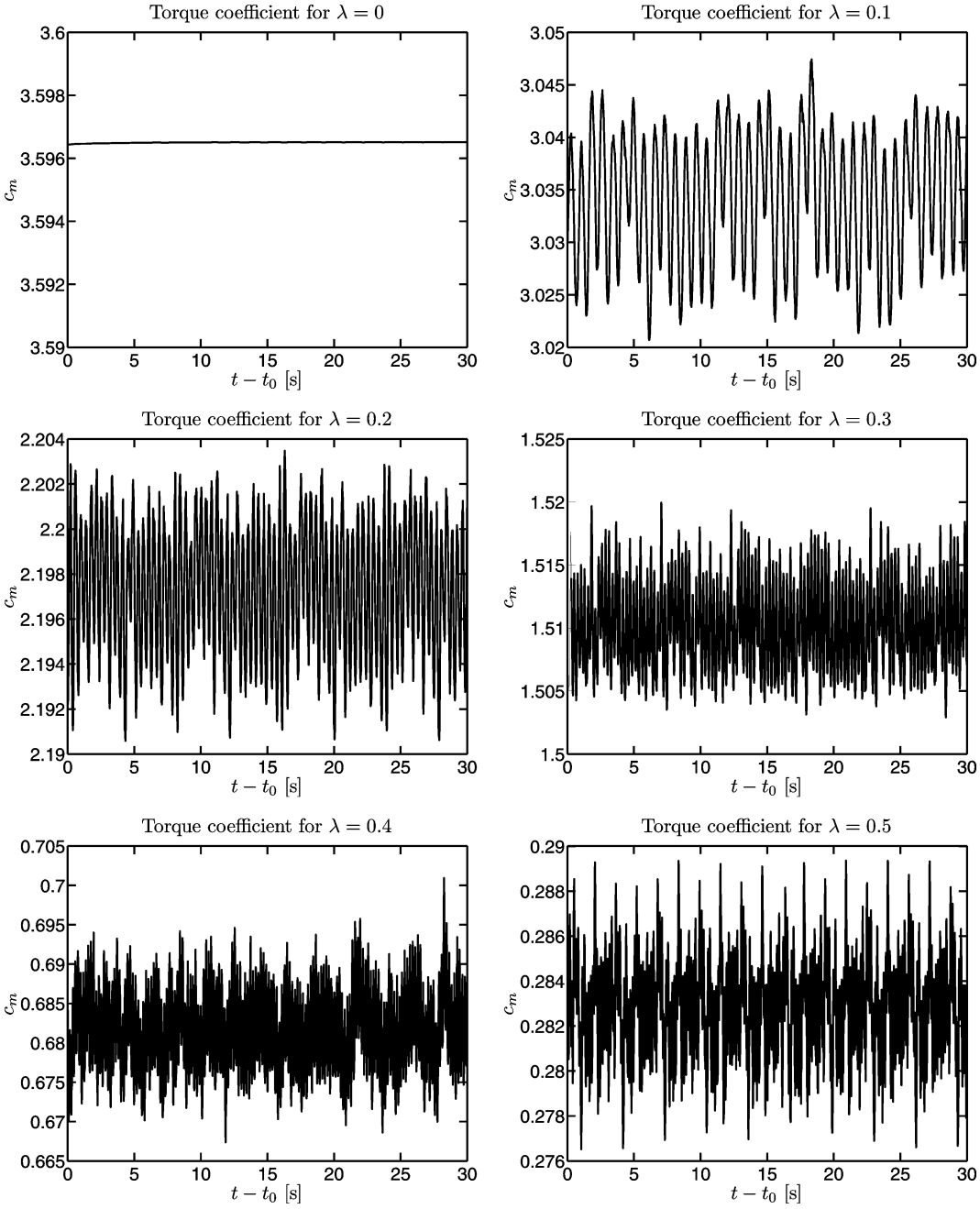

Fig. 6. Time variations of the torque coefficient at different tip speed ratios.

start of the turbine even under low wind speed conditions. As the tip speed ratio increases, the torque decreases and begins to oscillate around constant values. The amplitudes of the oscillations remain low, being smaller than 0.04 for all tip speed ratios. From the physical point of view, the main phenomena that can generate torque variations in time are the rotating movement of the runner and the vortex shedding behind the runner. From the point of view of numerical computations, up to a certain extent oscillations could also be introduced by the inherent numerical errors. Clearer explanations can be found by examining the frequency spectra of the torque coefficient oscillations. These spectra are presented in Fig. 7. It can be seen that for each tip speed ratio (except for $\lambda = 0$) the value of the dominant frequency increases as the tip speed ratio increases. Comparing the values on the plots with the frequencies in Table 1, it results that the values of the dominant frequencies equal the values f_b corresponding to the time intervals, in which the angle between two successive blades is swept. Thus, we can conclude that the main cause of torque oscillations resides in the periodic passage of the runner blades in front of a fixed arbitrary point.

As previously mentioned, numerical simulations were also performed for $\lambda = 0.6$. The torque coefficients obtained for this tip speed ratio have negative values showing that the machine operates no more as a wind turbine. This result suggests that the upper working limit of a wind turbine with crossflow runner is attained at a tip speed ratio between 0.5 and 0.6.

Time averaged values of the torque coefficients and of the corresponding power coefficients are plotted against the tip speed ratio in Fig. 8a and 8b, respectively. For comparison, variations of these coefficients found in literature [6, 7] for other wind turbine types are presented in Fig. 8c. The torque coefficient shows a nearly linear decrease as the tip speed ratio increases. This behaviour is quite similar to wind turbines based on drag forces, like the Savonius turbine, and to horizontal axis wind turbines having a large number of blades. From the point of view of the starting torque coefficient, the obtained results suggest that the wind turbine with crossflow runner is by far superior to other types of wind turbines. The power coefficients were computed starting from the formula [5]

$$c_p = \frac{P}{0.5\,\varrho\,v_\infty^3\,S}\,. \tag{3}$$

Knowing that the power has the expression $P = \omega\,M$ and substituting the torque as it results from equation (2), the following relationship can be obtained:

$$c_p = \lambda\,c_m\,. \tag{4}$$

This relationship was used to compute the values plotted in Fig. 8b. The peak power coefficient is obtained at a tip speed ratio that lies between 0.2 and 0.3. In this range,

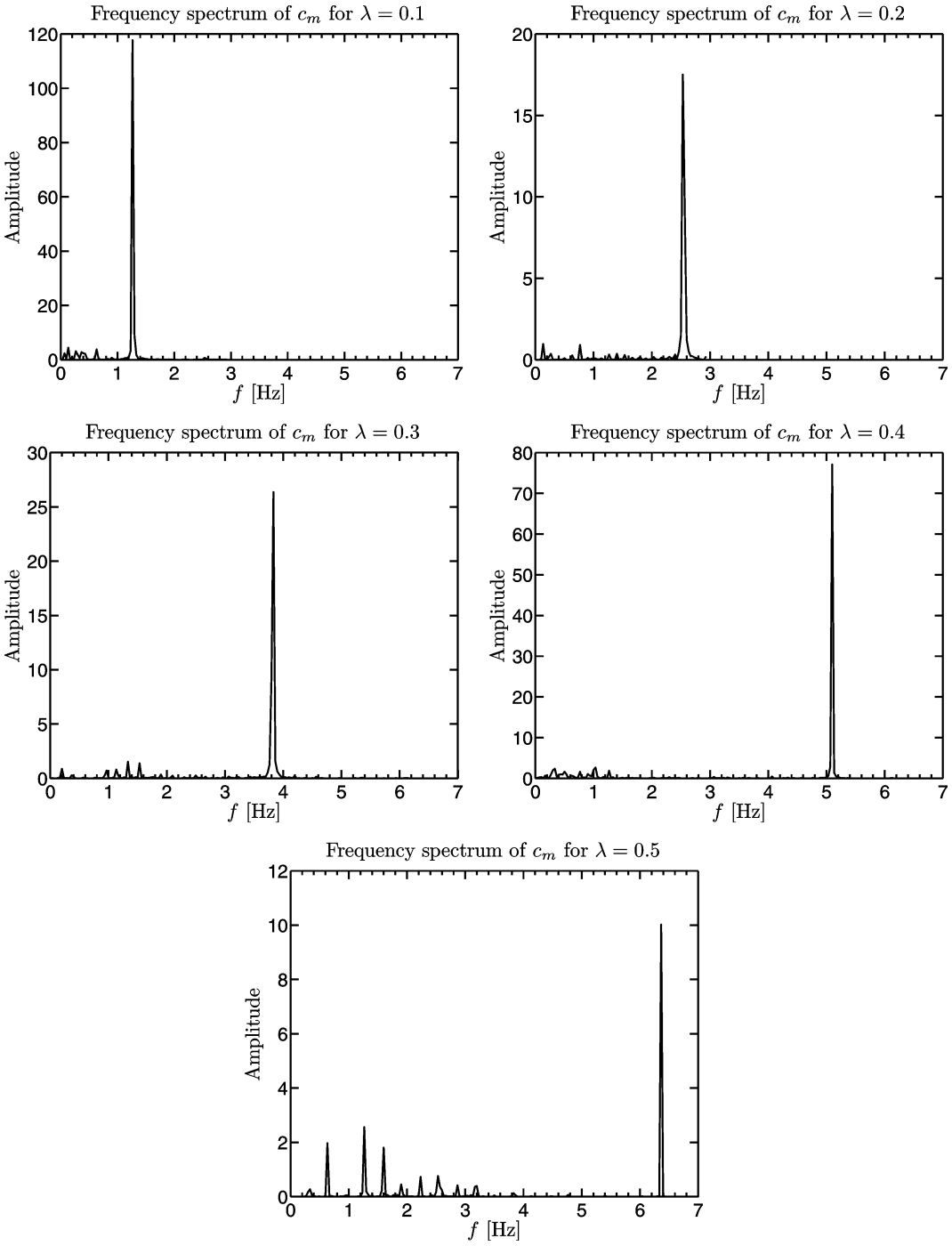

Fig. 7. Frequency spectra of torque coefficient variations at different tip speed ratios.

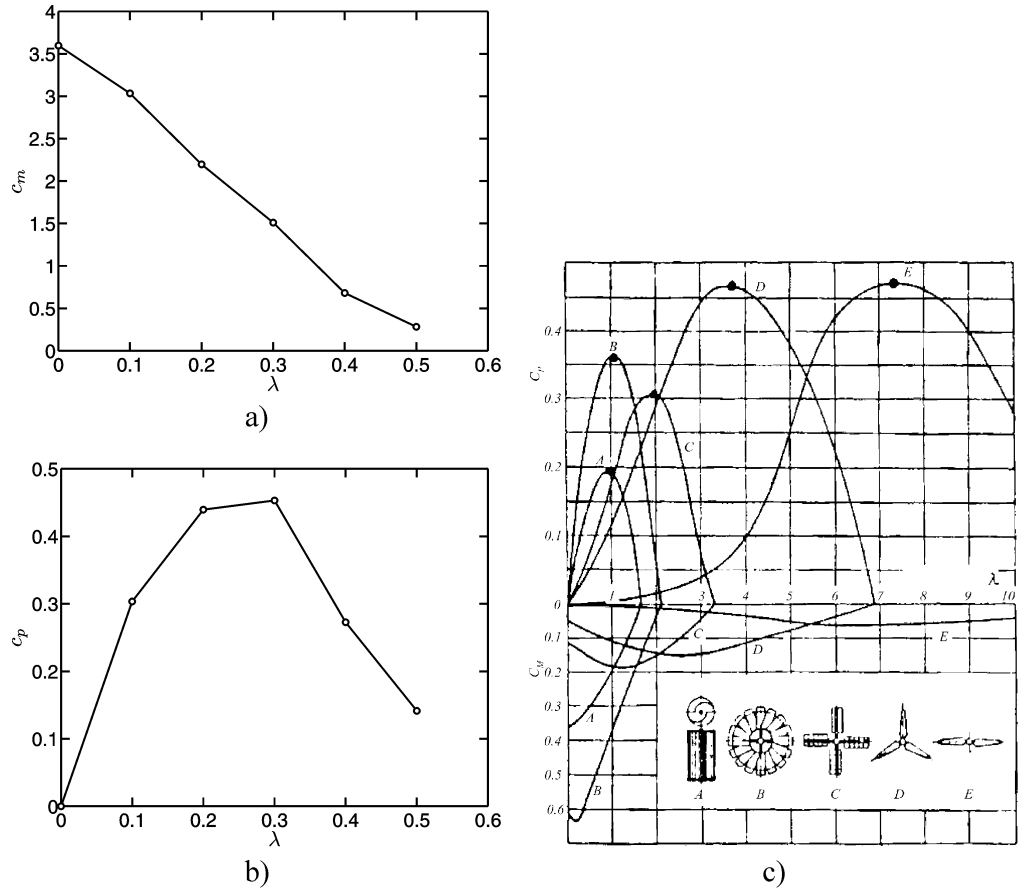

Fig. 8. Dependence of the torque coefficient (a) and power coefficient (b) on the tip speed ratio obtained by numerical simulations for the wind turbine with crossflow runner and variations of these coefficients presented in literature [6, 7] for other wind turbine types (c).

the power coefficient has values around 0.45. These values can be considered high if compared with the maximum theoretical value of near 0.6, which results from Betz' Theory, and with maximum values typical to other wind turbine types. It can be seen that the maximum values of the power coefficient are twice the maximum values attained by Savonius turbines and close to the maximum values obtained by horizontal axis wind turbines with two and three blades. The main disadvantage of the wind turbine with crossflow runner is that it has the narrowest working range compared to the other wind turbines, the maximum tip speed ratio that can be attained being less than 0.6. Because of this, if the turbine is ment for power generation, a gear box will probably be required in order to keep the electrical generator as small as possible and this will increase the overall cost and decrease the overall performance.

4. Conclusions

We studied a wind turbine with crossflow runner by numerical simulations in order to assess to what extent such a turbine could be efficient in low wind conditions. For the analyzed runner, with an outer diameter of 1 m, the obtained results suggest that the turbine can operate only in a relatively narrow range of tip speed ratios, the maximum tip speed ratio being lower than 0.6. The narrow operating range represents the main disadvantage of the turbines with crossflow runner. Nevertheless, the value of near 3.6 obtained for the starting torque coefficient is considerably higher than that of other wind turbine types. Due to this fact we can assume that the turbine is very fast starting even in low wind conditions, which represents an important advantage. Another advantage is that the turbine can attain a high power coefficient, of about 0.45, comparable to those of horizontal axis wind turbines.

Although the numerical results seem encouraging, experimental measurements are required to confirm them. If confirmed, the results recommend the wind turbine with cross flow runner for use in isolated areas having low wind conditions. The efficiency of the turbine could be further increased by using adequate wind concentrators, for example by placing the turbine horizontally on a roof top and enclosing in a properly designed casing those blades on which the wind has a breaking effect.

REFERENCES

[1] *A.K. Wright, D.H. Wood*, "The starting and low wind speed behaviour of a small horizontal axis wind turbine", in Journal of Wind Engineering and Industrial Aerodynamics, no. 92, 2004, pp. 1265-1279.

[2] *I.C. Mandiş, D.N. Robescu, M. Bărglăzan*, "Capitalization of wind potential using a modified Banki wind turbine", in UPB Scientifical Bulletin, Series D: Mechanical Engineering, **vol. 70**, no. 4, 2008, pp. 115-124.

[3] *C.A. Mockmore, F. Merryfield*, "The Banki Water Turbine", in Bulletin Series No. 25, Oregon State College, 1949.

[4] * * * Fluent 6.3 User's Guide, Fluent Inc., 2006.

[5] *M. Exarhu*, Maşini şi instalaţii hidraulice şi pneumatice (Hydraulic and pneumatic machinery and installations), ISBN 978-973-0-04409-6, Bucureşti, 2006 (in Romanian).

[6] *T. Ackerman, L. Söder*, "Wind Energy Technology and Current Status: a Review", in Renewable and Sustainable Energy Review, **vol. 4**, no. 4, 2000, pp. 315-374.

[7] *A.D. Şahin*, "Progress and Recent Trends in Wind Energy", in Progress in Energy and Combution Science, no. 30, 2004, pp. 501-543.